Solid State Phenomena
ISSN: 1662-9779, Vol. 390, pp 181-188
doi:10.4028/p-b48XNq
© 2026 The Author(s). Published by Trans Tech Publications Ltd, Switzerland.
Submitted: 2026-01-19
Revised: 2026-02-21
Accepted: 2026-02-21
Online: 2026-04-17

Mechanical Performance of a Steel-Polymer Biphasic Lattice Structure

Edoardo Mancini[1, a*], Anastasia Ciccarella[1,b], Andrea Di Giuliano[1,c], Lino Micarelli[1,d], Giuseppe Dell'Avvocato[1,e] and Katia Gallucci[1,f]

[1]Università degli Studi dell'Aquila, DIIIE, Piazzale Ernesto Pontieri I, 67100 L'Aquila, Italy

[a]edoardo.mancini@univaq.it, [b]anastasia.ciccarella@graduate.univaq.it, [c]andrea.digiuliano@univaq.it, [d]lino.micarelli@student.univaq.it, [e]giuseppe.dellavvocato@univaq.it, [f]katia.gallucci@univaq.it

Keywords: Biphasic lattice structure, homogenization, gyroid, polymer.

Abstract. Interpenetrating Phase Composites (IPCs) with biomimetic properties are promising materials for strengthening orthopaedic implants while also increasing their biocompatibility. Thanks to additive manufacturing techniques, lattice structures can be employed to develop biomaterials with controlled architectures, enabling the replication of human bone structures and offering advantages in terms of strength-to-weight ratio. This study investigates the behaviour of a bi-material steel-polymer lattice structure, observing that the epoxy resin increases the mechanical strength of gyroid, leaving the lightweight properties unchanged. Moreover, an equivalent constitutive model was calibrated, and a homogenization procedure based on the Representative Volume Element theory was applied. The effect on mechanical strength due to the 316L powder dispersed within the epoxy resin was investigated as well.

Introduction

The bio-inspired structures exhibit outstanding lightweight properties, strength, and toughness while optimizing material efficiency and mechanical performance [1]. Through a long evolutionary process, living organisms have developed in nature diverse biological structures, well-adapted to their environments [2]. Artificial biomimetic cellular structures are promising for biomedical applications, thanks to their high strength-to-weight ratio and tunable mechanical properties; these architectures, enhanced by Additive Manufacturing technologies, offer great potential for patient-specific medical devices.

The gyroid, one of the Triply Periodic Minimal Surfaces (TPMS), belongs to the cubic crystal system and was first described in [3]. Owing to its suitability for lightweight, high-strength applications, the gyroid structure has been extensively explored for the design of advanced materials that could be exploited in biomedical applications. Gyroid structures may be classified as either sheet-based or strut-based [4].

In this paper, the behaviour of a bi-material steel-polymer lattice structure was investigated as an Interpenetrating Phase Composite (IPC) with biomimetic properties: the steel part is constituted of a sheet-based gyroid cellular structures (designed and manufactured using Laser Powder Bed Fusion, L-PBF); the polymeric part consists of an epoxy resin that fills the gyroid cavities, optionally loaded with steel powder.

Parallelepiped samples were produced at laboratory scale and experimentally tested to identify mechanical behaviours, expressed in terms of engineering stress-strain curves. Experimental data were exploited to develop mathematical models able to reproduce the mechanical behaviour of the steel-polymer biphasic lattice structures: the elastic regime was interpreted by a homogenization procedure [5], to lower the computational effort of IPC simulations; the plastic regime was framed by a new-Three-Stage (newTS) Hollomon model [6] combined with an additional tailored power-law-term that simulates the densification stage [7].

This study might pave the way to the design of customized IPC prosthetic devices; the developed models might be used to verify the suitability of steel-polymer biphasic lattice structures to overcome the limitations related to the use of cemented protheses, e.g., in hip-joint-replacement.

This article is an open access article under the terms and conditions of the Creative Commons Attribution (CC BY) license (https://creativecommons.org/licenses/by/4.0)

Materials and Methods

Materials. Parallelepipedal samples were prepared at lab-scale (edges ~8 mm, Fig. 1): (i) Gyroid structures made of AISI 316L were 3D-printed by Laser Powder Bed Fusion; (ii) epoxy resin (FansArriche) was cast into the Gyroids, as such or mixed with 30 wt% of 316L powder (Sauter diameter 28 µm). The biphasic steel-polymer lattice cell was discretized using tetrahedral elements for the subsequent numerical homogenization (Fig. 1b).

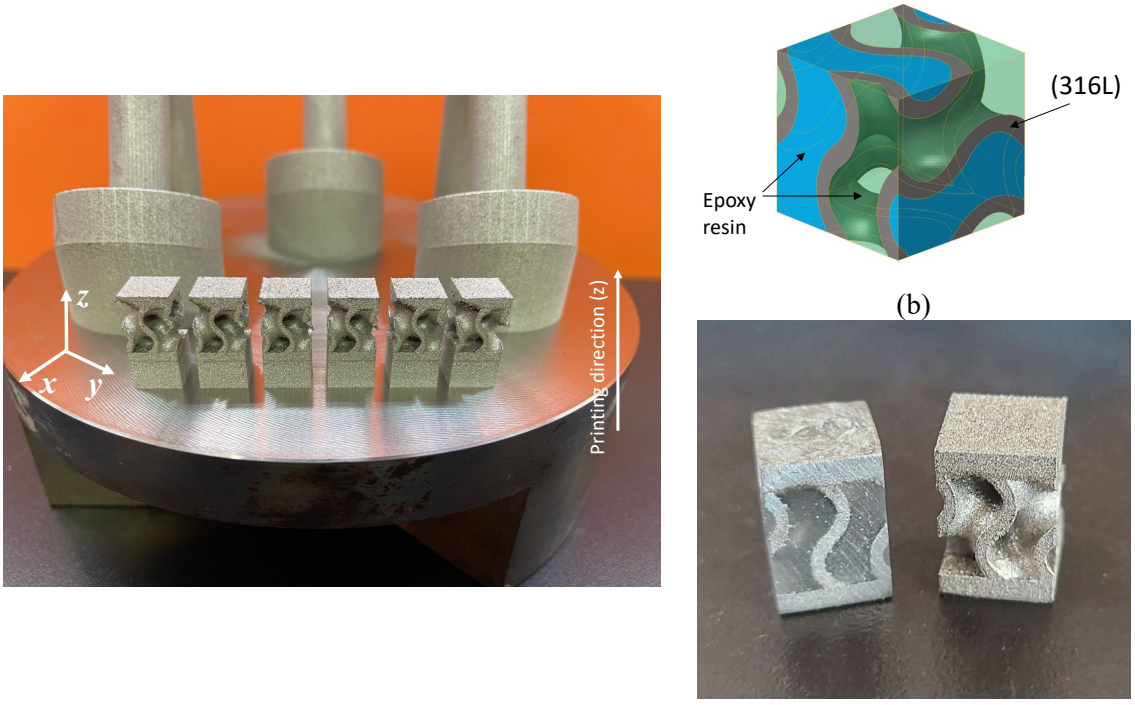

Fig. 1. Biphasic steel-polymer lattice structure: (a) Gyroid on building platform, (b) biphasic steel-polymer lattice cell FE Model and (c) samples with and without epoxy resin

Starting from the raw specimens (Fig. 1a), the samples underwent quasi-static compression tests and microstructural analysis. Both specimens with and without epoxy resin were tested (Fig. 1c).

The samples are labelled as **Sp1**, **Sp2**, and Sp3; Table 2 summarizes the samples' main features, i.e., with or without epoxy resin filling and optional addition of 316L powder to the resin.

Table 1. Summary of all samples

Specimen	+ epoxy resin	wt% of 316L powder	Cell Size [mm]	Sample size [mm]
Sp 1	-	-		
Sp 2	Yes	-	8x8x8	8x8x10
Sp 3	Yes	30%		

Equipment. Quasi-static compression tests were carried out using an MTS Universal servo-hydraulic testing machine (Fig. 2). All tests were performed under displacement-controlled conditions at a constant engineering strain rate of 10^{-3} s^{-1}.

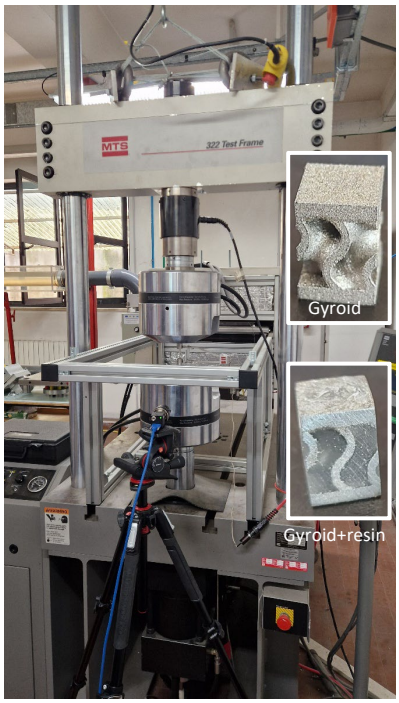

Fig. 2. Quasi-static test set-up: a Universal servo-hydraulic test machine and gyroid samples with and without epoxy resin

Numerical homogenization procedure. A mesoscale numerical homogenization was performed to identify the elastic stiffness matrix. Representative volume elements were analysed under six periodic loading conditions [7][8]. Tetrahedron elements with a minimum edge length of 0.15 mm were utilized. Figure 3 illustrates the six numerical models and their corresponding loading conditions. All biphasic samples exhibit periodic boundary conditions; for clarity, the epoxy resin is depicted solely in Fig. 3a. To account for the anisotropic effects of 3D printing, the anisotropic elastic matrix $[E_{ij}]_{base}$ of the base material was considered.

The procedure was applied only for the sample **Sp2** (Gyroid + epoxy resin).

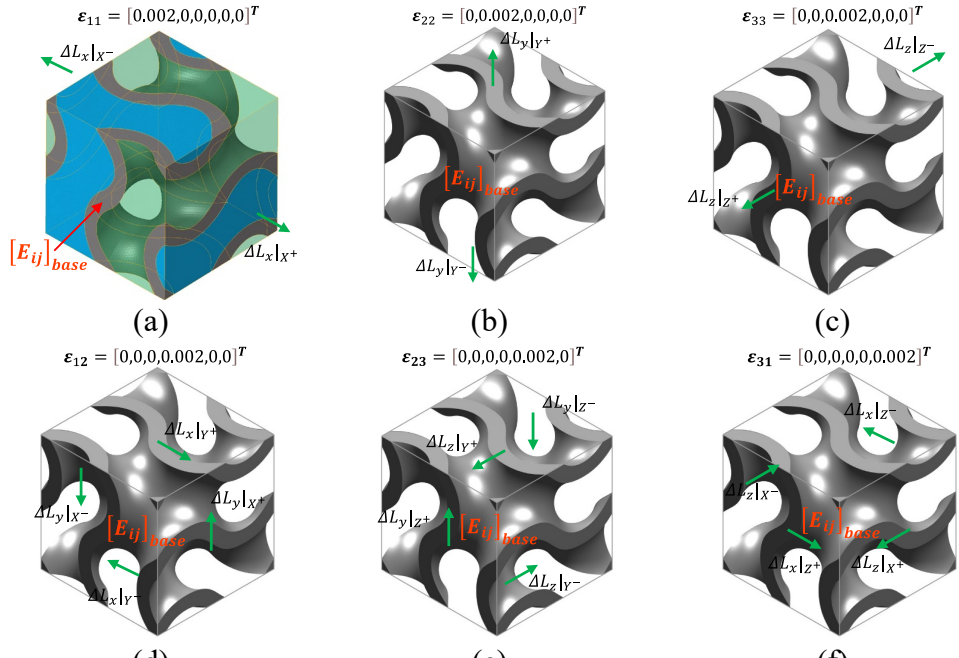

Fig. 3. Periodic loading conditions**:** (a) Cell size 8mm Gyroid RVEs with epoxy resin and (b) the six loadings

To identify the $[E_{ij}]_{base}$ experimental tests on 3D printed bulk samples were performed. The samples were produced with two different orientations relative to the Z-building direction (Fig. 4a) and tested under two load types: tension and torsion. This evaluation aimed to assess the effects of anisotropy by the matrix reported in Fig. 4b [8].

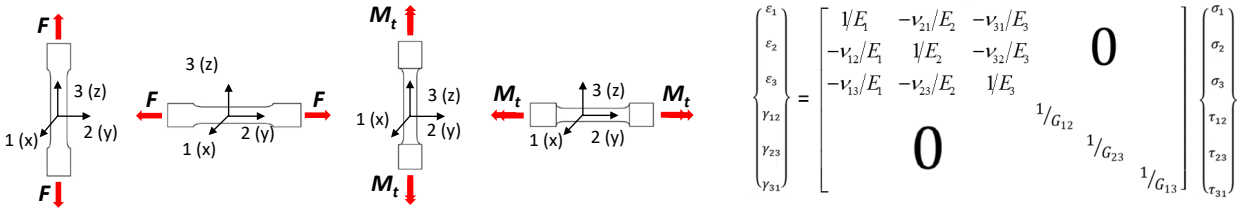

(a) (b)

Fig. 4. Stiffness anisotropic elastic matrix identification: **(a)** sample schematization with loading referred to Z-building direction, **(b)** anisotropic elastic matrix for transversally isotropic materials

Results and Discussion

Experimental Results. Fig. 5 shows the quasi-static experimental curves of all specimens. As to samples **Sp2** and **Sp3**, the curve profiles reveal a change in concavity in the strain interval between about 0.05 and 0.15, during which the curves tend to turn upward. At higher strains (@0.2), the work-hardening behaviour characterized by downward concavity is re-established, finally showing the cellular densification stage.

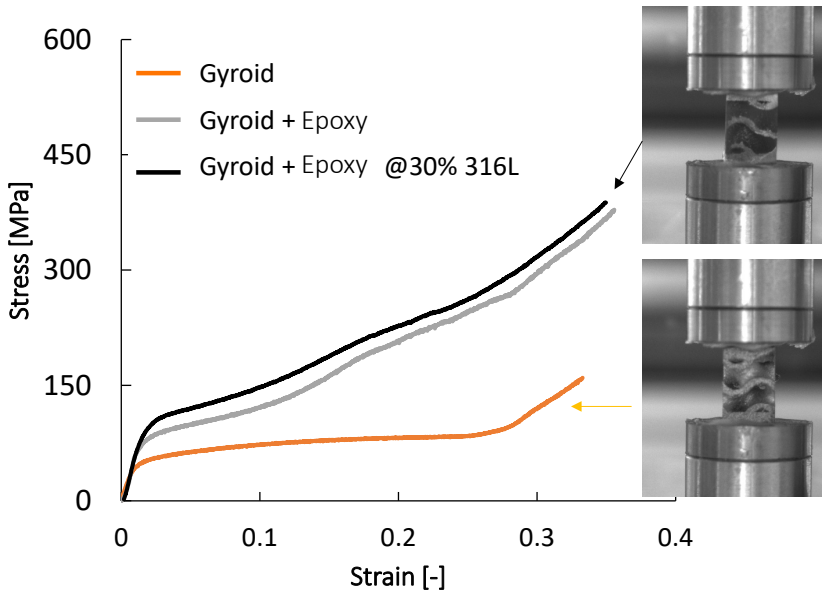

Fig. 5. Experimental results: Engineering stress-strain curves

Constitutive Modelling and Fitting. Different models are available in the literature to reproduce the experimental behaviour recorded during tests and shown in Fig. 5. For most metals, work-hardening is better illustrated on bi-logarithmic stress–strain charts than on linear plots. With σ and ε respectively representing engineering stress and strain, in the presence of a linear ln(ε)–ln(σ) relationship, the material behaviour may be effectively represented by the Hollomon power-law equation, $\sigma = K\varepsilon^n$; under these conditions, the slope of the bi-logarithmic plot is indicative of the strain-hardening exponent n, whereas the intercept at ε = 1 on the vertical axis corresponds to the strength coefficient K. The curve shown in Fig. 6 is obtained by plotting the quasi-static stress–strain data of the **Sp3** in Fig. 5 on a bi-logarithmic scale.

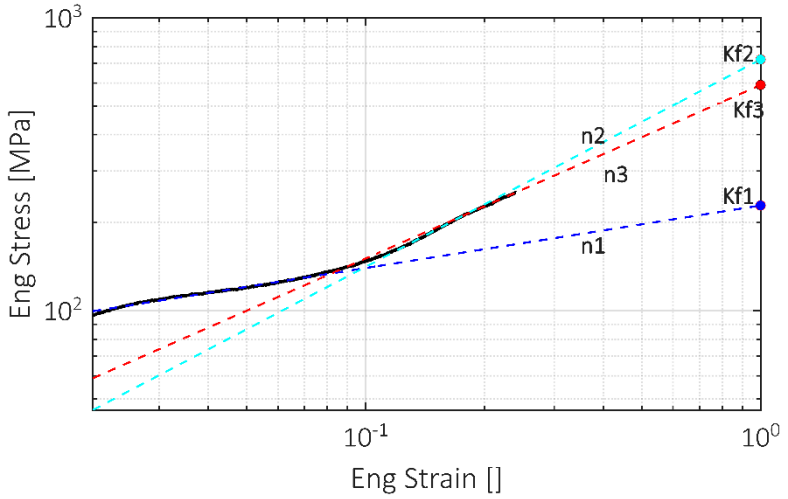

Fig. 6. Stress–true strain curve on the bi-logarithmic plane: Gyroid + Epoxy @30% 316L (Sp3)

The crossing points of the three linear regressions in Fig. 6 identify two threshold strains, ε_{t1} and ε_{t2}. These strain values represent a material parameter and can be employed to divide the Hollomon laws into TSs:

$$\begin{aligned} \sigma &= K_1\varepsilon^{n_1}, \quad && \varepsilon < \varepsilon_{t1} \\ \sigma &= K_2\varepsilon^{n_2}, \quad && \varepsilon_{t1} < \varepsilon < \varepsilon_{t2} \\ \sigma &= K_3\varepsilon^{n_3}, \quad && \varepsilon > \varepsilon_{t2} \end{aligned} \tag{1}$$

The strain hardening and strength coefficients could be made to vary continuously along with strain, leading to a modified Hollomon equation (Eq. 2).

$$\sigma = h \cdot K(\varepsilon)\varepsilon^{n(\varepsilon)} + A\left(\frac{\varepsilon}{1-\varepsilon}\right)^B \tag{2}$$

Variables σ and ε are engineering stress and strain, respectively, both considered positive in compression. h is the parameter that allows for moving from one curve to another at different powder percentages. The parameters K and n are expected to vary smoothly with strain, conferring to σ vs. ε curves an S-shaped trend characterised by asymptotic behaviour at both low and high strain levels, and a gradual transition around the threshold strains ε_t. A and B coefficients describe the densification region. Sigmoid function has been used to model the transition from the hardening stages.

Fig. 7 compares with experimental results of **Sp3** the following modelling output: (i) the quasi-static curve fitted using the newTS Hollomon model (black curve); the three distinct power-law relationships (dashed lines) corresponding to the different work-hardening phases, (iii) the second term of the new model (green curve).

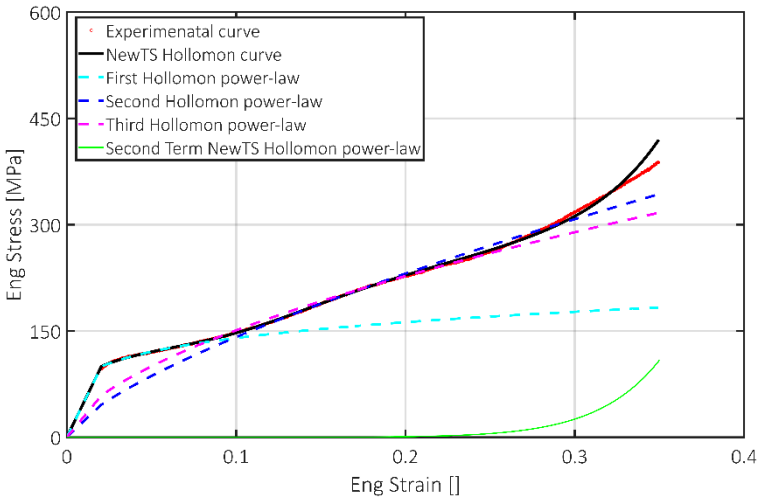

Fig. 7. Comparison between analytical and experimental curves of Sp3 sample: different contributions of each term of the model, Hollomon Power laws fitting and second term new model

Numerical homogenization results. Mesoscopic numerical models have been prepared on a biphasic unit cell 8x8x8 in order to identify the elastic matrix coefficients ($[E_{ij}]_{cell}$) of **Sp2**; this sample was chosen to test the homogenisation procedure on a simpler case, avoiding to introduce experimental uncertainties related to the spatial distribution of AISI 316L powder load in the resin. The results of the numerical homogenisation are expressed by the homogenized elastic stiffness matrix of Fig. 8a. Moreover, the Zener factor (Z_r) [9] was calculated to detect the anisotropic behaviour (Fig. 8b).

16229.6	6365.2	6617.6	-17.1	-254.5	15.1
	16382.3	6632.7	-19.5	-21.4	247.2
		17436.8	-262.3	-18.0	11.9
			4645.8	2.3	-29.0
				4854.1	-5.1
					4873.9

(a)

$$\frac{2E_{44}}{E_{11}-E_{12}} = 0.94$$

(b)

Fig. 8. Numerical homogenisation results of the Gyroid Biphasic Lattice Structure of Sp2: (a) Homogenized Elastic Stiffness Matrix $[Eij]_{cell}$ and (b) Zener ratio Z_r

Simulation results. Both mesoscale and macroscale of the biphasic steel-polymer Gyroid unit cell. The linear elastic-anisotropic material model $[E_{ij}]_{cell}$ for macroscale simulation was adopted. The Finite Element (FE) models are detailed in Fig. 9, rows "Boundary conditions" and "Discretization"; the results for von Mises equivalent stress are reported in Fig. 9 ("Results" row). To evaluate the anisotropy effect, two displacement loading conditions were applied in the Z and Y directions, respectively. Tetrahedron elements with minimum edge lengths of 0.15 mm and 0.25 mm were used for mesoscale and macroscale, respectively. The results confirmed the optimal homogenization process for the biphasic Gyroid in the elastic regime for quasi-static tests, reducing computational cost.

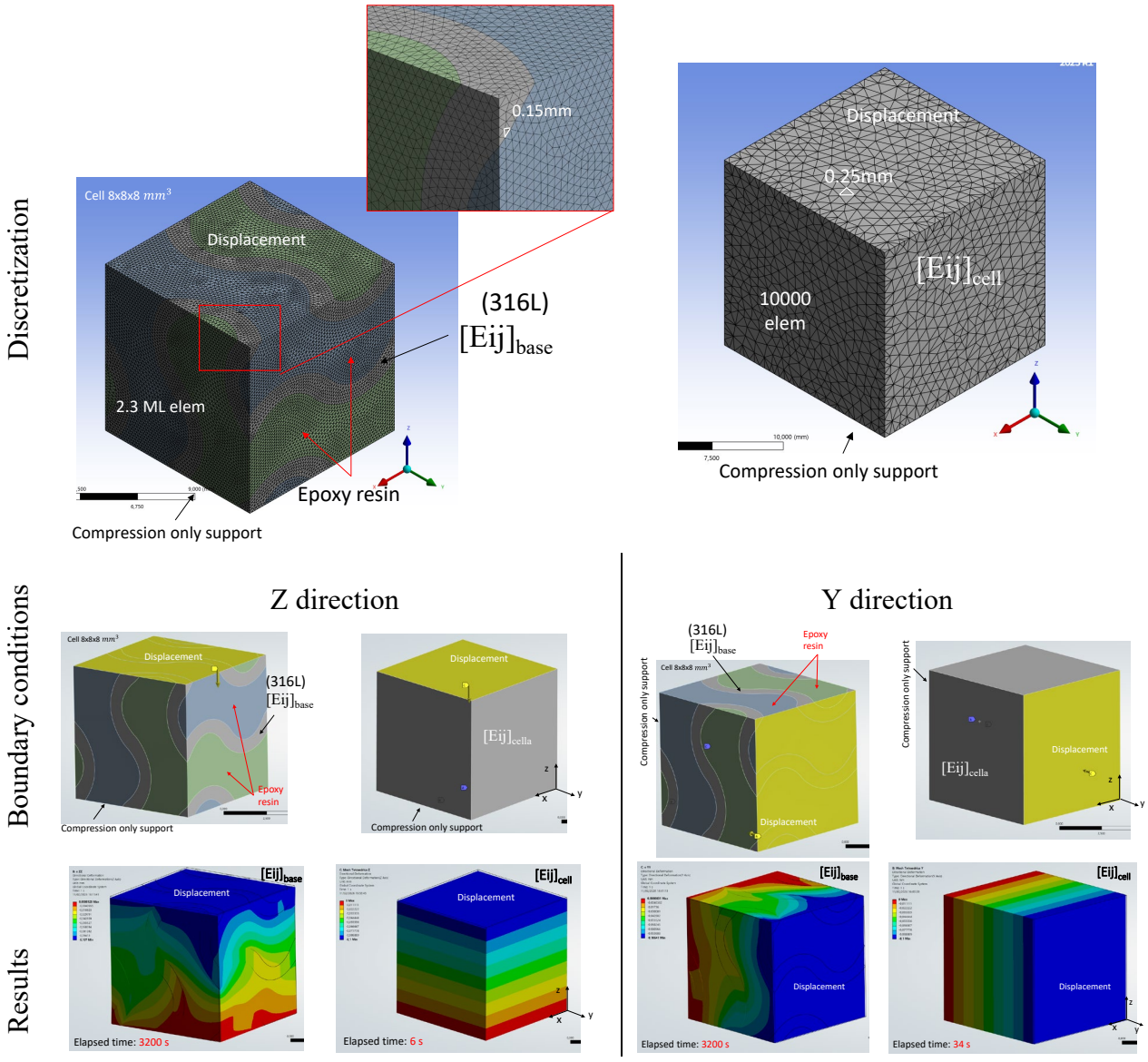

Fig. 9. FE model: Boundary conditions, discretization and results. (a, c) Mesoscale and (b, d) macroscale. "Discretization" line reports the cell size and elements number and minimum length. The stiffness comparison between meso and macro-scale are in the "Results" line

Conclusion

A biomimetic-inspired two-phase structure was studied. TPMS Gyroid was chosen as the lattice structure, and both epoxy resin and epoxy resin with the addition of AISI-316L-powder were used as fillers.

The most important findings can be summarized as follows:

- the epoxy resin increases the mechanical strength of the gyroid (Gyroid + Epoxy, Fig. 5), leaving the lightweight properties unchanged;
- a further increase in mechanical strength is due to the 316L powder added to the epoxy resin;
- the elastic regime has been reproduced by a homogenization procedure based on the Representative Volume Element theory;
- an alternative constitutive model, referred to as the "newTS Hollomon power-law", was developed to describe the biphasic lattice-structured material behaviour in the plastic regime.

Acknowledgement

The authors wish to thank Dr Luca Benerecetti for his help with material model calibration and Giuseppe Organtini for the experimental tests.

References

[1] L. Guo et al., Integrated biomimetic biphasic structures for high-strain-rate resistance and thermal insulation: Design, fabrication and performance characterization, Eng. Sci. Technol. Int. J. 67 (2025) https://doi.org/10.1016/j.jestch.2025.102088

[2] D. Ramakrishna, G. Bala Murali, Bio-inspired 3D-printed lattice structures for energy absorption applications: A review, Proc. Inst. Mech. Eng., Part L: J. Mater. Design Appl. 237 (3) (2022) 503–542.

[3] H. Shoen, Alan, Infinite Periodic Minimal Surface without Intersections, NASA. (1970).

[4] D. Li, W. Liao, N. Dai, Y.M. Xie, Absorption of Sheet-Based and Strut-Based Gyroid, Materials (Basel). (2019)

[5] E. Mancini, M. Utzeri, E. Farotti, A. Lattanzi, and M. Sasso, "DLP printed 3D gyroid structure: Mechanical response at meso and macro scale," Mechanics of Materials, vol. 192, May 2024.

[6] M. Utzeri et al., Quasi-Static and Dynamic Behavior of Inconel 625 Obtained by Laser Metal Deposition: Experimental Characterization and Constitutive Modeling, J. Eng. Mater. Technol. 143 (2021) DOI: 10.1115/1.4051087

[7] E. Mancini et al. Definition of a unified material model for cellular materials with high morphological and topological dispersion: Application to an AA7075-T6 aluminium foam, Materials Science & Engineering A, 833 (2022) https://doi.org/10.1016/j.msea.2021.142346

[8] Ciccarella, A., Dell'Avvocato, G., Cortis, G., & Mancini, E. (2025). Meso-and macroscale modelling strategies for biomimetic structures produced using L-PBF technology. Material Forming: ESAFORM 2025, 313.

[9] C.M. Zener, S. Siegel, Elasticity and Anelasticity of Metals, J. Phys. Colloid Chem. 53 (1949) 1468–1468.